1 **CRISPR screening identifies novel PARP inhibitor classification based on**

2 **distinct base excision repair pathway dependencies**

3

4 Gregory A. Breuer[1,2], Jonathan Bezney[1], Nathan R. Fons[1,2], Ranjini K. Sundaram[1], Wanjuan

5 Feng[3], Gaorav P. Gupta[3], and Ranjit S. Bindra[1,2,*]

6

7 [1] Department of Therapeutic Radiology, Yale University School of Medicine, New Haven, CT

8 06520-8034, USA

9 [2] Department of Pathology, Yale University School of Medicine, New Haven, CT 06520-8034,

10 USA

11 [3] Department of Radiation Oncology, University of North Carolina, Chapel Hill, 27599

12

13 *To whom correspondence should be addressed. Email: ranjit.bindra@yale.edu

14

15

16

17

18

19

20

21 **ABSTRACT**

22 DNA repair deficiencies have become an increasingly promising target for novel therapeutics

23 within the realm of clinical oncology. Recently, several inhibitors of Poly(ADP-ribose)

24 Polymerases (PARPs) have received approval for the treatment of cancers primarily with

25 deleterious mutations in the homologous recombination (HR) proteins, BRCA1 and BRCA2.

26 Despite numerous clinical trials which have been completed or are currently ongoing, the

27 mechanism of action by which PARP inhibitors selectively kill tumor cells is poorly

28 understood. While many believe "trapping" of PARP proteins to DNA at sites of damage is

29 the most important determinant driving cytotoxicity by these drugs, clinically effective

30 inhibitors exist with a diverse range of PARP-trapping qualities. These findings suggest that

31 characterization of inhibitors as strong versus weak trappers does not properly capture the

32 intra-class characteristics of these drugs. Here, we use a novel, targeted DNA damage

33 response (DDR) CRISPR/Cas9 screening library to reveal heterogenous genetic dependencies

34 on the base excision repair (BER) pathway for PARP inhibitors, which is not correlated with

35 PARP trapping ability or catalytic inhibition of PARP. These findings demonstrate that

36 inhibition of PARylation and induction of PARP trapping are not the only factors contributing

37 to distinct biological activity for different PARP inhibitors, and they provide insight into the

38 optimal choice of PARP inhibitors for use in the setting of specific DDR defects.

39

40 **AUTHOR SUMMARY**

41 Targeted cancer therapies rely on our general understanding of which genetic mutations are

42 involved in both sensitivity and resistance to such anticancer agents. In this study, we

43 describe the use of functional genetic screening to evaluate the role of various DNA repair

44 proteins in response to inhibitors of PARP, a quintessential example of targeted therapy.

45   While PARP inhibitors are best known for their utility in cancers with homologous

46   recombination defects, we show that some inhibitors within this class may have additional

47   functionality in cancers with deficient base excision repair. These findings highlight not only

48   the importance of PARP inhibitor selection in the appropriate context, but also the

49   mechanistic differences that exist within this class of inhibitors. It is our hope that our

50   findings will inspire future work evaluating the use of specific PARP inhibitor selection in

51   designing clinical trials to further expand the use of PARP inhibitors beyond tumors with

52   homologous recombination deficiencies.

53

54   **INTRODUCTION**

55   Over the last decade, inhibitors of poly(ADP-ribose) polymerase-1 and -2 (PARP1/2) have

56   been established as safe and effective cancer therapeutics, which are most active against

57   tumors with homologous recombination (HR) defects, such as those with deleterious

58   mutations in BRCA1, BRCA2, and others [1-3]. The PARP family of proteins utilize NAD+ to

59   add one (mono-) or more (poly-) ADP-ribose chains to target proteins in response to various

60   stimuli (referred to as PARylation) [4]. While most proteins downstream from PARP1 and

61   PARP2 act in DNA damage response (DDR) pathways, over 170 different PARP interactions

62   have been described, and thus these proteins play important roles in a diverse range of

63   functions, ranging from cell cycle regulation to cell motility [5, 6]. Furthermore, the targets

64   of such PARylation events are known to be stimulus-dependent [7]. PARP proteins play a

65   well-established role in single strand break (SSB) repair, in which they recruit proteins such

66   as XRCC1 and other factors for resolution of these lesions [8]. Prevention of SSB repair can

67   result in increased replication stress, unrepaired double-strand breaks (DSBs), and difficulty

68   with replication restart, which collectively are thought to underlie the enhanced cytotoxicity

69   of PARP inhibitors in HR-defective cancers [9-11]. However, recent evidence suggests that

70   the effect of "trapping" PARP1 at sites of SSB repair may be more important for cytotoxicity

71   of these agents, particularly in HR-defective cells [12, 13]. Trapping has been exhibited for

72   both PARP1 and PARP2, though PARP1 remains the most important family member

73   regarding SSB repair and the induction of synthetic lethality [8]. Despite these new insights,

74   clinically relevant PARP inhibitors exist across a wide spectrum of potencies and specificities,

75   in relation to PARP trapping ability, catalytic inhibition of PARylation, and efficacy in

76   targeting other members of the PARP family of proteins [14]. Additionally, loss of PARP

77   function in the setting of HR deficiencies shows moderate growth inhibition, independent of

78   trapping inhibitors, indicating that both actions may be important for cell toxicity [15].

79

80   More recent studies suggest that synthetic lethal interactions with PARP inhibitors extend

81   beyond BRCA1 and BRCA2 mutations, to including additional DDR proteins, such as

82   mutations in the RAD51 paralogues, PALB2, ATM, and others [16]. Furthermore, PARP

83   inhibitor sensitivity has been used as a screening tool to identify novel HR-related functions

84   of genes, such as mutant IDH1 and ribonuclease H2 [17, 18]. As *in vitro* studies continue to

85   show an ever-expanding landscape of possible uses for PARP inhibitors, it is not fully

86   understood whether these sensitivities extend across the entire class of PARP inhibitors, or

87   only a subset of drugs within this class.

88

89   With the knowledge that PARP trapping ability is functionally independent of catalytic

90   inhibition, we set out to characterize the utility of the clinically available inhibitors --

91   olaparib, rucaparib, talazoparib, niraparib, and veliparib. Using a high coverage, targeted

92   DDR CRISPR/Cas9-based screening library, we have developed a novel assay focused solely

93   on known DDR modulators for greater sensitivity and reproducibility. In addition, we have

94   characterized the most clinically relevant PARP inhibitors based on inhibition of PARylation

95   and PARP1 trapping ability, in order to look for patterns of induced sensitivity to PARP

96   inhibition in the presence of key DDR defects. We report here that clinically relevant PARP

97   inhibitors can be functionally clustered into two unique classes, based on activity in the

98   presence of base excision repair (BER) defects, and not on PARP1 trapping ability as was

99   previously suggested. These results show that effectors of response to PARP inhibitors

100   extend beyond the scope of HR perturbation and PARP trapping, and suggests that a better

101   understanding of secondary targets may be critical for the optimal application of the

102   numerous PARP inhibitors which are now being used in the clinic.

103

104   **RESULTS**

105   **Clinically-relevant PARP inhibitors have varying degrees of specificity for PARP1 trapping**

106   **and inhibition of PARylation**

107   PARP inhibitors have traditionally been evaluated via qualitative or quantitative

108   immunoassays measuring downstream PARylation in the setting of induced DNA damage.

109   We adapted this format to 96-well microplates to better accommodate high-throughput

110   quantification, and to more accurately parallel the methods used in short-term viability

111   assays using the same compounds (**Fig 2A**). We tested a diverse and structurally unique

112   collection of PARP inhibitors in these studies (**Fig 1**). As expected, all PARP inhibitors showed

113   dose-dependent inhibition of PARylation in the setting of alkylation damage, with a nearly

114   1000-fold difference between the most potent inhibitor of PARylation, talazoparib, and the

115   weakest tested, A-966492 (**Fig 2B**).

116

117   We then tested the same panel of inhibitors in a fluorescence polarization-based assay,

118   which measures binding of PARP1 to a fluorescently-labeled DNA substrate in the presence

119   and absence of PARP inhibition [12]. As expected, measured polarization of wells containing

120   compounds reported to have strong PARP-trapping characteristics showed increased

121   potency when compared to compounds such as veliparib, which have been reported to have

122   limited trapping potency (**Figs S1A-B**). Similar to results from measured inhibition of

123   PARylation, talazoparib was again found to be the most potent compound tested in the

124   fluorescence polarization assay, with a measured IC50 approximately 10-fold lower than the

125   next most potent compound (**Fig 2C**). Additional results were found to correlate well with

126   previously published data [12, 19]. Notably, potency of PARP inhibitors as measured by

127   PARylation immunoassay was not found to be significantly correlated with trapping potency

128   as measured by PARP1 trapping assay (R^2 = 0.1058, p > 0.05, Spearman r = 0.3), indicating

129   that these two processes occur independent of one another (**Fig 2D**).

130

131   **Both PARP1 trapping potency and inhibition of PARylation fail to independently predict**

132   **synthetic lethality in HR-deficient cells**

133   As noted earlier, synthetic lethal interactions between PARP1 inhibition and HR-deficiencies

134   are hypothesized to be markedly enhanced by trapping of PARP1 at sites of DNA damage

135   [20]. In order to quantify growth inhibition across all tested PARP inhibitors, we performed

136   short-term viability assays in isogenic HR-proficient and -deficient colorectal

137   adenocarcinoma cell lines, DLD-1 and DLD-1 BRCA2-/-, respectively. Growth inhibition in

138   both cell lines across the spectrum of PARP inhibitors was found to vary widely relative to

139   the IC50s for PARylation and PARP1 trapping (**Fig 3A,B**). Growth inhibition in the HR-

140   proficient DLD-1 cell line was found to be significantly correlated with both inhibition of

141 PARylation (p = 0.006) and trapping potency (p < 0.0001) (**Fig 3A**). However, growth

142 inhibition in HR-deficient DLD-1 BRCA2-/- cells was not found to correlate with inhibition of

143 PARylation (p = 0.345) and only trended towards a significant correlation with trapping

144 potency (p = 0.068) (**Fig 3B**). Interestingly, specific growth inhibition in HR-deficient cells

145 relative to wild-type counterparts did not correlate with either inhibition of PARylation (p =

146 0.4384) or PARP1 trapping (p = 0.7213) (**Fig 3C**). Overall, these findings suggest that neither

147 the inhibition of PARylation, nor the PARP trapping ability of PARP inhibitors independently

148 predicts the magnitude of synthetic lethality of PARP inhibitors in HR-deficient cell lines.

149

150 **Targeted CRISPR/Cas9 screen reveals a novel classification of PARP inhibitors**

151 Numerous prior studies have elucidated synthetic lethal interactions between PARP

152 inhibition and specific DNA repair deficiencies (reviewed in [21]), while few have focused on

153 possible differences between multiple structurally unique PARP inhibitors and DDR genes.

154 We thus performed a targeted CRISPR/Cas9-based lentiviral screen using five structurally

155 unique inhibitors from **Fig 1**, which were selected to represent the broad range of PARP

156 trapping and PARylation activities that we observed in our earlier studies (see **Figs 4A,B**).

157

158 To evaluate the validity and sensitivity of our assay, analysis of all tested PARP inhibitors

159 were combined in comparison to DMSO-treated control group, with the expectation that

160 key proteins involved in homologous recombination would be among the most sensitizing

161 findings. Among the top single-gene knockouts conferring sensitivity to all tested PARP

162 inhibitors were RAD51, XRCC3, BRCA1, RNF8, ATM, ATR, and others (**Fig 4C**). Knockout of

163 PARP1 was also shown to confer a general resistance to PARP inhibition as expected, though

164 the size of this effect varied depending on the specific inhibitor in question. Individual PARP

165   inhibitors were generally well-correlated with the average response to PARP inhibitors, with

166   talazoparib being most similar to the average (R^2 = 0.7307) and veliparib and rucaparib (R^2 =

167   0.61, 0.614) being least correlated to the average response (**Fig S2**).

168

169   In order to look for trends in response to single-gene knockouts across multiple inhibitors,

170   dimensionality reduction was performed, using response to each gene as input. Using these

171   techniques, compounds showing similar responses across our targeted library should cluster

172   closer together. Principal components analysis of inhibitors based on response to single-

173   gene knockouts revealed two groupings of clinical PARP inhibitors, with Group A consisting

174   of talazoparib, olaparib, and niraparib and Group B consisting of veliparib and rucaparib (**Fig**

175   **4D**). These data suggest a novel division of clinically relevant PARP inhibitors based entirely

176   on functional classification in response to deficiencies in DNA repair, and does not appear to

177   correlate with measured inhibition of PARylation or PARP1 trapping potency (**Fig 3A-C**).

178

179   **Group-specific targets reveal response to XRCC1, LIG3, and PARP1 knockout as key**

180   **predictors of overall potency of PARP inhibitors**

181   To better evaluate the defining characteristics between Group A and Group B inhibitors, we

182   used publicly available gene ontology data to look for differences in effect of key DDR

183   pathways. Although HR and Fanconi Anemia pathways showed the strongest sensitizing

184   phenotype to both Group A and Group B inhibitors, differences between the two groups

185   were best exemplified by differences in sensitization to key proteins in both base excision

186   repair (BER) and mismatch repair (MMR) pathways (**Fig 5A**). Within BER, increased

187   resistance to PARPi in the presence of PARP1 knockout and increased sensitivity to PARPis

188   upon loss of LIG3 and XRCC1 were the most defining characteristics of Group A inhibitors

189   relative to others (**Fig 5B**). Increased sensitivity to POLE4 was also noted among Group A

190   inhibitors followed by differential sensitivities to FEN1, LIG1, and PARP3 approaching

191   significance (**Fig 5B**).

192

193   Findings from the initial screen were confirmed first by testing selected sgRNAs from the

194   original library by 96h short-term viability assay and then by pooled siRNA experiments to

195   measure the effect of knockdown, rather than knockout, of each gene in the presence of

196   PARPi. Short-term viability assays were also performed using U2-OS cells to show effects

197   carry across unrelated cell lines, independent of tissue of origin. Both individual sgRNA

198   experiments, as well as siRNA experiments, largely recapitulated the results seen by pooled

199   CRISPR/Cas9 screening (**Figs 6A-C, Fig S3**). XRCC1 and LIG3 knockouts and knockdowns show

200   increased sensitivity to Group A inhibitors that are far less pronounced or absent in Group B

201   across all assays. These findings confirm the results from our targeted CRISPR/Cas9 screen,

202   showing that loss of function of XRCC1 and LIG3 confer increased sensitivity to some, but

203   not all PARP inhibitors. Interestingly, sensitization to PARP inhibition has been shown

204   previously in the setting of XRCC1 deficiency, however this study was limited only to the

205   Group A inhibitors, talazoparib and olaparib [22]. Additionally, the degree of sensitization in

206   the setting of loss of either XRCC1 and LIG3 appears to correlate with the overall PARP1-

207   dependence of toxicity, and may provide critical insight into better understanding the

208   therapeutic effects of PARP inhibition in the setting of such deficiencies.

209

210   **In *silico* analysis reveals similar clustering of tested PARP inhibitors and association with**

211   **PARP1/XRCC1/LIG3 loss-of-function**

212   To assess our functional genetic screening methods in comparison to alternative datasets,

213   we examined publicly available datasets from the DepMap project comparing gene

214   essentiality and drug sensitivity across hundreds of human cell lines. Interestingly, principal

215   components analysis of the relative sensitivities of each of the five examined PARP

216   inhibitors tested across over 400 cell lines reveals clusters coinciding with those found via

217   our functional genetic screen, with higher degrees of correlation between talazoparib,

218   niraparib, and olaparib than with rucaparib and veliparib (**Fig 7A**). We next performed

219   hierarchical clustering to identify groupings of cell lines with similar sensitivity patterns to

220   the tested inhibitors to examine qualities relating to selective sensitivity in talazoparib,

221   niraparib, and olaparib (**Fig 7B**). Notably, cell lines with relative sensitivity to PARP inhibition

222   were split between two groups - the pan-sensitive group identified as Cluster 1 and the

223   selectively sensitive group identified as Cluster 3. Cell lines within Cluster 3 are defined by

224   moderate to high sensitivity to talazoparib, niraparib, and olaparib and mid to low sensitivity

225   to rucaparib and veliparib (**Fig 7C**).

226

227   We next performed an analysis of gene essentiality within each cluster to measure what

228   factors correlate with pan-sensitivity rather than selective sensitivity. Analysis of relative

229   sensitivity to loss of selected genes identified within our functional screen as well as genes

230   having a significant cluster-dependent effect via ANOVA analysis (**Fig 7D**). Cell lines

231   exhibiting pan-sensitivity to PARP inhibition in Cluster 1 are more sensitive to loss of FEN1,

232   LIG1, PARP1, and PARP2, but not LIG3 or XRCC1 in comparison to cell lines showing selective

233   sensitivity in Cluster 3. Such differences between pan-sensitive and selectively sensitive cell

234   lines may provide insight into the differing mechanism resulting in cytotoxicity in the

235   presence of PARP inhibition.

236

237   **DISCUSSION**

238   While the exact mechanistic basis for synthetic lethal interactions with PARP inhibition in

239   the setting of BRCA1/2 mutations and HR deficiencies remains controversial, our data

240   clearly demonstrate that neither trapping potency nor strength of inhibition of PARylation

241   fully explain the response to such inhibitors. These findings are in agreement with recent

242   biochemical studies suggesting that inhibitors of PARP1 fit into three major classifications

243   based on allosteric effects of PARPi binding as well as retention at sites of DNA damage [23].

244   Similarly, our unbiased analysis of over 280 genes known to be involved in DNA damage

245   repair and response found unique groupings of PARP inhibitors which do not correlate solely

246   with either the ability to inhibit downstream PARylation by PARP1 or the trapping of PARP1

247   to sites of damage based on widely-used biochemical assays. Across the PARP inhibitors

248   tested in our analysis, we do not observe any correlation between synthetic lethality in the

249   context of HR defects and strength of PARP1 trapping or inhibition of PARylation. Indeed,

250   PARP trapping has been associated with increased toxicity in both normal tissue as well as

251   within tumors, likely resulting in side effects seen in clinical trials such as complete bone

252   marrow failure and other cytopenias [24]. Such findings make appropriate classification of

253   inhibitors for use in patient populations ever more relevant, as the use of PARP inhibitors in

254   clinic becomes increasingly common.

255

256   Within our screen, we see strong sensitization to all PARP inhibitors through knockout of

257   key components of HR (RAD51, BRCA1, BRCA2, etc.), however only three of our tested

258   inhibitors respond to loss of function of proteins immediately downstream of PARP1 in BER.

259   Interestingly, loss of XRCC1 and LIG3 was found to be most toxic to cells concurrently

260   treated with inhibitors that are dependent on PARP1 for sensitization (Group A PARP

261   inhibitors). We hypothesize that this observation may be due to one or more of the

262   following mechanisms. i) PARP1-independent inhibitors may be maximally disrupting

263   downstream BER through disruption of PARP1 signaling at lethal doses, so further loss of

264   function does not alter response to inhibition. ii) Loss of XRCC1 and LIG3 results in

265   hyperactivation of PARP1 as has been shown previously, and is therefore increasing

266   opportunities for PARP1-dependent toxicity [25]. iii) Loss of XRCC1 and LIG3 results in

267   unrepaired lesions of the DNA, which may be preferentially targeted by PARP1-dependent

268   inhibitors. Differential sensitivity to loss of function of PARP1, PARP2, LIG1, and FEN1 as

269   seen in our DepMap essentiality analysis indicates that all PARP inhibitors may be equally

270   effective in targeting cells dependent on BER function, however talazoparib, niraparib, and

271   olaparib may have extended functionality outside of this scope. Additional work is necessary

272   to tease apart such mechanisms and further evaluate the utility of various classes of PARP

273   inhibitors in specific clinical settings.

274

275   Although there are over 250 active clinical trials testing PARP inhibitors in cancer at the time

276   of this writing, there is little information regarding appropriate selection of PARP inhibitor

277   therapy and utilization of PARP inhibitors in patients who have failed to respond to one or

278   more of such inhibitors. Likewise, no head-to-head clinical trials comparing PARP inhibitors

279   have been completed to date, making selection of PARP inhibitor treatment in the clinical

280   setting difficult. Neither PARP trapping nor catalytic inhibition of PARylation appear to

281   explain the efficacy of PARP inhibition in the treatment of cancers with DNA repair

282   deficiencies. Our results indicate that the efficacy of PARP inhibitors may hinge on some

283   combination of PARP trapping and inhibition of downstream targeting of PARP1, with a

284   handful of inhibitors, talazoparib > niraparib > olaparib, being far more dependent on the

285   presence of PARP1 than others. Clinical trials are necessary to determine the utility of

286   PARP1-independent inhibitors in the setting of limited PARP1 expression. Additionally,

287   patients with mutations in XRCC1 and LIG3 may benefit from treatment with talazoparib,

288   olaparib, or niraparib over treatment with PARP1-independent inhibitors. Further studies

289   are necessary to determine how these results may affect response to treatment in patients,

290   and whether our findings may translate into a clinical setting. Overall, our results highlight

291   an exciting technique in functional analysis of PARP inhibition via CRISPR/Cas9 screening to

292   define genetic dependencies, and show the importance of functional BER in the setting of

293   select PARP inhibitors.

294

295   **MATERIALS AND METHODS**

296   ***Cell lines and reagents***

297   Colorectal adenocarcinoma cell lines DLD-1 and DLD-1 BRCA2 -/- were used and maintained

298   in RPMI medium with 10% fetal bovine serum (FBS; Gibco) at 37ºC with 5% CO_2. The DLD-1

299   BRCA2$^{-/-}$ cell line has an engineered exonic deletion as described [26]. HEK293FT

300   (ThermoFisher) are human embryonal kidney cells maintained in Dulbecco's Modified

301   Eagle's Medium, high glucose (DMEM; Thermo Scientific/Gibco) supplemented with 10%

302   FBS. MCF10A cells are normal human mammary cells and were maintained in DMEM/F12

303   media (Gibco, #11330032) supplemented with 5% horse serum, 10 ng/ml epidermal growth

304   factor, 0.5 mg/ml hydrocortisone, 100 ng/ml cholera toxin, and 10 ug/ml insulin. PARP

305   inhibitors tested for the purposes of this study were obtained from the following vendors:

306   Talazopoarib (Selleckchem; #S7048), olaparib (Selleckchem; #S1060), rucaparib

307   (Selleckchem; #S1098), niraparib (Selleckchem; #S2741), veliparib (Selleckchem; #S1004), A-

308   966492 (Selleckchem; #S2197), KU-0058948 (Axon Medchem; #2001), NMS-P118

309   (Selleckchem; #S8363), E-7449 (Selleckchem; #S8419), AG-014699 (Axon Medchem; #1529),

310   BGB-290 (BeiGene).

311

312   ***PARylation Immunoblot***

313   To measure PARylation inhibition, MCF10A cells were plated on 96-well microplates

314   (Greiner) at a density of 20k cells/well 24h prior to treatment with methyl-

315   methanesulfonate (MMS; Sigma) and indicated PARP inhibitors. After 24h in culture, media

316   from the plates was aspirated and a fresh 75 µl of pre-warmed media was added to each

317   well. To this, 25 µl of media containing either 0.01% MMS, PARP inhibitors, or a combination

318   of the two were added to each well. Cells were incubated for 30m in normal culture

319   conditions. Following the 30m culture, media was aspirated and cells were rinsed once with

320   PBS. Cell cultures were lysed with RIPA lysis buffer for 30m at 4ºC with occasional agitation.

321   Lysates were spotted on nitrocellulose membrane (BioRad) and allowed to dry at room

322   temperature for 1h. Blocking was performed in TBS-T with 5% BSA (Gold Biotechnology) for

323   1h at room temperature, followed by overnight incubation with anti-PAR antibody

324   (Trevigen, #4336-BPC-100) at 4ºC. After primary incubation, three 10-minute washes with

325   TBS-T were performed, followed by 1h incubation with HRP anti-rabbit conjugated

326   secondary antibody (ThermoFisher; #31462) at room temperature under constant agitation.

327   Images obtained on ChemiDoc (BioRad) following addition of Clarity Western ECL substrate

328   (BioRad). Image quantification was done using ImageJ imaging software and normalized to

329   no-MMS and no-PARPi control [27]. Curve fitting and data analysis performed using

330   Graphpad Prism (Graphpad Software).

331

PARP1 Trapping Assay

Preparation of PARP1 dsDNA substrate was performed as previously described [28]. Briefly,

single-stranded oligonucleotides were hybridized by combining in equimolar ratio of the

following sequences:

5'-AlexaFluor488-ACCCTGCTGTGGGCdUGGAGAACAAGGTGAT

ATCACCTTGTTCTCCAGCCCACAGCAGGGT

This mixture was then heated to 95 ºC for 5m and slowly cooled to room temperature at 5

ºC/min. Hybridized oligonucleotide was then incubated with APE1 and UDG (NEB) at 37ºC

for 1h to create a single strand break recognized by the PARP1 enzyme.

To measure inhibition of release of DNA substrate from PARP1 enzyme, 30 nM GST-Tagged

PARP1 protein (BPS Biosciences) was incubated with 1 nM DNA substrate and varying

amounts of PARPi or DMSO for 1h in reaction buffer containing 50 mM Tris (pH 8.0), 4 mM

$MgCl_2$, 10 mM NaCl, and 50 ng/ml BSA in water at RT. After 1 hour, fluorescence

polarization readings were recorded using a Cytation 3 (Biotek) multi-mode imager with

fluorescence polarization filter prior to adding 1mM NAD+ and every 5 minutes after. Curve-

fitting and statistical analysis was performed using Graphpad Prism (Graphpad Software).

The concentration of PARP1 to fluorescent dsDNA substrate was first titrated to optimize

detection of polarization via automated plate reader in 96-well half volume microplates (**Fig

S1**). To measure trapping efficiency of various PARP inhibitors, purified PARP1 protein, DNA

substrate, and varying concentrations of PARP inhibitors were incubated for 1h at room

temperature to ensure saturated binding capacity. After the incubation, NAD+ was added to

the reaction to initiate release of DNA from PARP1, and polarization measurements were

355   recorded in 5-minute intervals for 120 minutes. Importantly, controls lacking NAD+, PARP1

356   protein, and DNA substrate were included for normalization.

357

358   ***CRISPR/Cas9 Screening and Analysis***

359   A CRISPR/Cas9 DDR targeted library was assembled using available gene ontology databases

360   and lists of genes involved in DNA damage repair and response. The top 10 suggested

361   sgRNAs targeting each gene were selected from the http://www.genome-engineering.org/

362   website and supplemented with non-targeting control sgRNAs [29]. These oligos were

363   assembled into the LentiCRISPRv2 lentivirus backbone as described in the original protocols

364   [30, 31]. Viral production was carried out in HEK293FT cells by equimolar co-transfection of

365   LentiCRISPRv2 library, psPAX2, and pCMV-VSV-G using Lipofectamine 2000 (Invitrogen;

366   #11668027). lentiCRISPR v2 was a gift from Feng Zhang (Addgene plasmid # 52961), psPAX2

367   was a gift from Didier Trono (Addgene plasmid # 12260), and pCMV-VSV-G was a gift from

368   Bob Weinberg (Addgene plasmid # 8454) [32]. Viral titer was assessed upon collection and

369   concentration of lentiviral supernatant with Lenti-X Concentrator (Takara Biotech; #631231).

370   Appropriate final concentrations were chosen to maintain MOI < 0.3 to reduce probability of

371   coinfection with two or more sgRNA sequences. For screening, DLD-1 cells were transduced

372   in 8 μg/ml Polybrene (Sigma-Aldrich) with the multiplexed CRISPR/Cas9 library containing 10

373   unique sgRNAs targeting 284 different genes involved or implicated in DDR-associated

374   pathways along with one thousand non-targeting sgRNA controls. Cells were then selected

375   with Puromycin (InvivoGen; #ant-pr-1) for 3 days following transduction, ensuring a MOI <

376   0.3 to prevent multiple sgRNA integrations per cell. After initial selection, cells were split

377   into six treatment groups and treated with appropriate PARPi at calculated GI_{30} or DMSO as

378   indicated to assess effects on both sensitivity and resistance to tested inhibitors. Samples

379   were taken at Day 0 as well as every 2 days to ensure logarithmic growth while maintaining

380   a high sample size.

381

382   Preparation and sequencing of samples was conducted using dual-indexed paired-end

383   sequencing on MiSeq System (Illumina) using a 2x150 protocol. Library preparation was

384   conducted two independent primer sets. Primers used in the first reaction amplify the

385   targeted sgRNA region of the integrated vector and primers used in the second reaction

386   allow for indexing and multiplexing during sequencing. Additional spacer sequences of 0-2

387   bases were inserted between the adapter and sequence-specific portions of the sequencing

388   primers to increase library diversity during sequencing.

389   Analysis was performed using a rank scoring algorithm similar to one previously described

390   [33]. sgRNAs were extracted from sequencing reads, counted, and normalized to total

391   sample size and non-targeting control abundance. A rank score was calculated for each gene

392   represented in the targeted library by comparing the abundance of each sgRNA to its

393   representation in the targeting library sample. Each screen was done in duplicate and

394   samples were prepared from multiple time points in each treatment group to reduce

395   sampling error.

396

397   ***Short-Term Viability Assays***

398   Short-term viability assays validating individual sgRNA results were performed by first

399   transducing cells in 6-well plates with lentivirus, selecting with Puromycin for 48h, then

400   plating into 96-well plates for 24h prior to adding appropriate concentrations of PARPi. 96h

401   after the initiation of treatment, media was aspirated, cells were washed once with PBS and

402   were then fixed using 4% formaldehyde (Sigma-Aldrich) in PBS solution for 15m at room

403   temperature. Cells were then stained with Hoechst 33342 (Sigma-Aldrich; #B2261) for 45

404   minutes prior to imaging using the Cytation 3 multi-mode imager as described previously

405   [34]. Cell counting was performed using a pipeline created in CellProfiler image analysis

406   software which stitches images by well and identifies the number of cell nuclei per well by

407   fluorescence staining [35]. Graphing and data analysis was performed using Graphpad Prism

408   (Graphpad Software). Assays utilizing pooled siRNA (Horizon; ON TARGETplus siRNA) were

409   conducted by first transfecting with RNAiMAX (Invitrogen; #13778100) 72h prior to

410   exposure to individual PARP inhibitors to ensure maximum knockdown at initial treatment.

411

412   ***In Silico Analysis of Drug Sensitivities and Gene Essentiality***

413   Gene essentiality data, drug sensitivity data, and accompanying cell line information was

414   obtained via the DepMap Data Portal (https://depmap.org/portal/download/) with

415   preprocessing steps as described in accompanying manuscripts [36-39]. Additional data

416   processing, dimensionality reduction, and plotting was done via Scikit-Learn [40].

417

418   **ACKNOWLEDGEMENT**

421

422   **REFERENCES**

423
424 1.   Farmer H, McCabe N, Lord CJ, Tutt AN, Johnson DA, Richardson TB, et al. Targeting the DNA
425   repair defect in BRCA mutant cells as a therapeutic strategy. Nature. 2005;434(7035):917-21.
426 2.   Ashworth A. A Synthetic Lethal Therapeutic Approach: Poly(ADP) Ribose Polymerase
427   Inhibitors for the Treatment of Cancers Deficient in DNA Double-Strand Break Repair. Journal
428   of Clinical Oncology. 2008;26(22):3785-90.
429 3.   Lord CJ, Ashworth A. PARP inhibitors: Synthetic lethality in the clinic. Science.
430   2017;355(6330):1152-8.
431 4.   Malanga M, Althaus FR. The role of poly(ADP-ribose) in the DNA damage signaling network.
432   Biochem Cell Biol. 2005;83(3):354-64.

433   5.   Isabelle M, Moreel X, Gagné J-P, Rouleau M, Ethier C, Gagné P, et al. Investigation of PARP-
434   1, PARP-2, and PARG interactomes by affinity-purification mass spectrometry. Proteome
435   Science. 2010;8:22-.
436   6.   Vyas S, Chesarone-Cataldo M, Todorova T, Huang Y-H, Chang P. A systematic analysis of the
437   PARP protein family identifies new functions critical for cell physiology. Nature Communications.
438   2013;4:2240.
439   7.   Jungmichel S, Rosenthal F, Altmeyer M, Lukas J, Hottiger Michael O, Nielsen Michael L.
440   Proteome-wide Identification of Poly(ADP-Ribosyl)ation Targets in Different Genotoxic Stress
441   Responses. Molecular cell. 2013;52(2):272-85.
442   8.   Fisher AEO, Hochegger H, Takeda S, Caldecott KW. Poly(ADP-Ribose) Polymerase 1
443   Accelerates Single-Strand Break Repair in Concert with Poly(ADP-Ribose) Glycohydrolase.
444   Molecular and Cellular Biology. 2007;27(15):5597-605.
445   9.   Kuzminov A. Single-strand interruptions in replicating chromosomes cause double-strand
446   breaks. Proceedings of the National Academy of Sciences of the United States of America.
447   2001;98(15):8241-6.
448   10.   Colicchia V, Petroni M, Guarguaglini G, Sardina F, Sahun-Roncero M, Carbonari M, et al. PARP
449   inhibitors enhance replication stress and cause mitotic catastrophe in MYCN-dependent
450   neuroblastoma. Oncogene. 2017;36(33):4682-91.
451   11.   Ronson GE, Piberger AL, Higgs MR, Olsen AL, Stewart GS, McHugh PJ, et al. PARP1 and
452   PARP2 stabilise replication forks at base excision repair intermediates through Fbh1-
453   dependent Rad51 regulation. Nature Communications. 2018;9(1):746.
454   12.   Murai J, Huang SY, Das BB, Renaud A, Zhang Y, Doroshow JH, et al. Trapping of PARP1 and
455   PARP2 by Clinical PARP Inhibitors. Cancer research. 2012;72(21):5588-99.
456   13.   Pommier Y, O'Connor MJ, de Bono J. Laying a trap to kill cancer cells: PARP inhibitors and
457   their mechanisms of action. Sci Transl Med. 2016;8(362):362ps17.
458   14.   Carney B, Kossatz S, Lok BH, Schneeberger V, Gangangari KK, Pillarsetty NVK, et al. Target
459   engagement imaging of PARP inhibitors in small-cell lung cancer. Nature Communications.
460   2018;9(1):176.
461   15.   Bryant HE, Schultz N, Thomas HD, Parker KM, Flower D, Lopez E, et al. Specific killing of
462   BRCA2-deficient tumours with inhibitors of poly(ADP-ribose) polymerase. Nature.
463   2005;434(7035):913-7.
464   16.   Schmitt A, Knittel G, Welcker D, Yang T-P, George J, Nowak M, et al. ATM Deficiency Is
465   Associated with Sensitivity to PARP1- and ATR Inhibitors in Lung Adenocarcinoma. Cancer
466   research. 2017;77(11):3040-56.
467   17.   Sulkowski PL, Corso CD, Robinson ND, Scanlon SE, Purshouse KR, Bai H, et al. 2-
468   Hydroxyglutarate produced by neomorphic IDH mutations suppresses homologous
469   recombination and induces PARP inhibitor sensitivity. Science Translational Medicine.
470   2017;9(375).
471   18.   Zimmermann M, Murina O, Reijns MAM, Agathanggelou A, Challis R, Tarnauskaite Z, et al.
472   CRISPR screens identify genomic ribonucleotides as a source of PARP-trapping lesions.
473   Nature. 2018;559(7713):285-9.
474   19.   Hopkins TA, Shi Y, Rodriguez LE, Solomon LR, Donawho CK, DiGiammarino EL, et al.
475   Mechanistic Dissection of PARP1 Trapping and the Impact on In Vivo Tolerability
476   and Efficacy of PARP Inhibitors. Molecular Cancer Research. 2015;13(11):1465-77.
477   20.   Ström CE, Johansson F, Uhlén M, Szigyarto CA-K, Erixon K, Helleday T. Poly (ADP-ribose)
478   polymerase (PARP) is not involved in base excision repair but PARP inhibition traps a single-
479   strand intermediate. Nucleic acids research. 2011;39(8):3166-75.
480   21.   Pilié PG, Gay CM, Byers LA, O'Connor MJ, Yap TA. PARP Inhibitors: Extending Benefit Beyond
481   BRCA-Mutant Cancers. Clinical Cancer Research. 2019;25(13):3759-71.
482   22.   Ali R, Alabdullah M, Alblihy A, Miligy I, Mesquita KA, Chan SYT, et al. PARP1 blockade is
483   synthetically lethal in XRCC1 deficient sporadic epithelial ovarian cancers. Cancer Letters.
484   2020;469:124-33.
485   23.   Zandarashvili L, Langelier MF, Velagapudi UK, Hancock MA, Steffen JD, Billur R, et al.
486   Structural basis for allosteric PARP-1 retention on DNA breaks. Science. 2020;368(6486).
487   24.   Hopkins TA, Ainsworth WB, Ellis PA, Donawho CK, DiGiammarino EL, Panchal SC, et al.
488   PARP1 Trapping by PARP Inhibitors Drives Cytotoxicity in Both Cancer Cells and Healthy Bone
489   Marrow. Molecular Cancer Research. 2019;17(2):409-19.
490   25.   Hoch NC, Hanzlikova H, Rulten SL, Tétreault M, Komulainen E, Ju L, et al. XRCC1 mutation is
491   associated with PARP1 hyperactivation and cerebellar ataxia. Nature. 2017;541(7635):87-91.

26. Hucl T, Rago C, Gallmeier E, Brody JR, Gorospe M, Kern SE. A Syngeneic Variance Library for Functional Annotation of Human Variation: Application to BRCA2. Cancer research. 2008;68(13):5023-30.

27. Rueden CT, Schindelin J, Hiner MC, DeZonia BE, Walter AE, Arena ET, et al. ImageJ2: ImageJ for the next generation of scientific image data. BMC Bioinformatics. 2017;18(1):529.

28. Murai J, Huang S-yN, Das BB, Renaud A, Zhang Y, Doroshow JH, et al. Trapping of PARP1 and PARP2 by Clinical PARP Inhibitors. Cancer research. 2012;72(21):5588-99.

29. Cong L, Ran FA, Cox D, Lin S, Barretto R, Habib N, et al. Multiplex Genome Engineering Using CRISPR/Cas Systems. Science. 2013;339(6121):819-23.

30. Sanjana NE, Shalem O, Zhang F. Improved vectors and genome-wide libraries for CRISPR screening. Nature methods. 2014;11(8):783-4.

31. Shalem O, Sanjana NE, Hartenian E, Shi X, Scott DA, Mikkelson T, et al. Genome-scale CRISPR-Cas9 knockout screening in human cells. Science. 2014;343(6166):84-7.

32. Stewart SA, Dykxhoorn DM, Palliser D, Mizuno H, Yu EY, An DS, et al. Lentivirus-delivered stable gene silencing by RNAi in primary cells. RNA. 2003;9(4):493-501.

33. Li W, Xu H, Xiao T, Cong L, I Love M, Zhang F, et al. MAGeCK enables robust identification of essential genes from genome-scale CRISPR/Cas9 knockout screens2014. 554 p.

34. Fons NR, Sundaram RK, Breuer GA, Peng S, McLean RL, Kalathil AN, et al. PPM1D mutations silence NAPRT gene expression and confer NAMPT inhibitor sensitivity in glioma. Nature Communications. 2019;10(1):3790.

35. Kamentsky L, Jones TR, Fraser A, Bray M-A, Logan DJ, Madden KL, et al. Improved structure, function and compatibility for CellProfiler: modular high-throughput image analysis software. Bioinformatics. 2011;27(8):1179-80.

36. DepMap B. DepMap 20Q4 Public. Figshare2020.

37. Dempster JM, Rossen J, Kazachkova M, Pan J, Kugener G, Root DE, et al. Extracting Biological Insights from the Project Achilles Genome-Scale CRISPR Screens in Cancer Cell Lines. bioRxiv. 2019:720243.

38. Meyers RM, Bryan JG, McFarland JM, Weir BA, Sizemore AE, Xu H, et al. Computational correction of copy number effect improves specificity of CRISPR-Cas9 essentiality screens in cancer cells. Nature genetics. 2017;49(12):1779-84.

39. Corsello SM, Nagari RT, Spangler RD, Rossen J, Kocak M, Bryan JG, et al. Discovering the anticancer potential of non-oncology drugs by systematic viability profiling. Nature Cancer. 2020;1(2):235-48.

40. Pedregosa F, Varoquaux G, Gramfort A, Michel V, Thirion B, Grisel O, et al. Scikit-learn: Machine Learning in Python. J Mach Learn Res. 2011;12(null):2825–30.

527   **FIGURE CAPTIONS**

528   **Fig 1. Chemical structures of selected PARPi.** Highlighted in red is the 3-aminobenzamide -

529   like structure which is thought to block PARP function via inhibition of NAD+ binding.

530

531   **Fig 2. Biochemical characterization of PARPi shows limited correlation between inhibition**

532   **of PARylation and PARP trapping** (A) Representative example of PARylation immunoassay

533   in MCF10A cells in presence and absence of 0.01% MMS and increasing amounts of the

534   PARP inhibitor olaparib. (B) Catalytic inhibition of PARylation EC_{50} as measured by

535   PARylation immunoassay +/- SEM. (C) PARP1 trapping EC_{50} per agent as measured by

536   fluorescence polarization assay +/- SEM. (D) Comparison of PARP1 trapping potency and

537   catalytic inhibition of PARylation.

538

539   **Fig 3. Synthetic lethality in HR-deficient cells shows no correlation with inhibition of**

540   **PARylation nor PARP trapping potency alone.** (A) Correlation between PARP1 trapping

541   potency or inhibition of PARylation with growth inhibition in HR-proficient and -deficient

542   DLD-1 cells. Correlation between growth inhibition in HR-proficient cells and inhibition of

543   PARylation was significant (R^2 = 0.2277; p = 0.006), as was correlation with PARP1 trapping

544   potency (R^2 = 0.53, p < 0.0001). (B) In DLD-1 BRCA2$^{-/-}$ cells, there was no observed

545   correlation between growth inhibition and inhibition of PARylation (R^2 = 0.0298, p = 0.345),

546   and correlation with PARP1 trapping only trended towards significance (R^2 = 0.107, p =

547   0.068). (C) Synthetic lethality does not correlate with either strength of inhibition of

548   PARylation or trapping potency.

549

550 **Fig 4. Targeted CRISPR screen reveals two unique functional groups of PARPi based on**

551 **overall response to loss of DDR genes.** (A) Visual representation of logIC50 values for

552 trapping potency, inhibition of PARylation, and growth inhibition in HR-proficient and -

553 deficient DLD-1 cells. (B) Summary of results from A. (C) Rank order average of tested

554 inhibitors over entire screening set with single-gene knockouts conferring increased

555 sensitivity or resistance highlighted at the extremes. (D) Principal components analysis of

556 tested inhibitors reveals two distinct groups of inhibitors with talazoparib, olaparib, and

557 niraparib making up Group A and veliparib, rucaparib making up Group B.

558

559 **Fig 5. Inter-group variation in response to PARPi shows greatest difference in genes**

560 **associated with BER.** (A) Comparison of group-averaged rank score by associated pathway.

561 Higher rank scores are associated with increased sensitivity to loss of function of proteins

562 within each reported pathway. A single gene may appear in more than one pathway. (B)

563 Per-gene rank scoring by PARPi group reveals significant differences in PARP1, LIG3, XRCC1,

564 and POLE4 response to inhibitors (p<0.0001, p=0.0094, 0.0004, and 0.047 via student's t-

565 test). Additional genes involved in base excision repair approaching significance include

566 FEN1, LIG1, and PARP3 (p=0.054, 0.062, 0.093).

567

568 **Fig 6. Loss of XRCC1 and LIG3 increase sensitivity to Group A inhibitors with limited effect**

569 **to Group B.** (A) Short-term viability assays reveal specific response to PARP1, LIG3, and

570 XRCC1 seen from CRISPR/Cas9 screen. Strong resistance in presence of PARP1 knockout also

571 associated with increased sensitivity in presence of XRCC1, LIG3 knockout. (B) Pooled siRNA

572 knockdown of each of the reported genes shows similar phenotype to CRISPR/Cas9 lentiviral

573 knockout; again showing increased sensitivity to talazoparib, olaparib, and niraparib in the

574   presence of XRCC1/LIG3 disruption. (C) Short-term viability assays in U2-OS cell line shows

575   similar phenotype with lentiviral CRISPR/Cas9 knockout of reported genes.

576

577   **Fig 7. Gene essentiality and drug sensitivity studies from DepMap dataset confirm**

578   **functional clustering of PARPi and dependence on BER pathway.** (A) Principal components

579   analysis of DepMap sensitivities to tested PARP inhibition shows clustering similar to those

580   seen via PCA of our functional genetic screen with talazoparib, olaparib, and niraparib

581   having similar effects across cell lines in comparison to rucaparib and veliparib. (B) Principal

582   components analysis and agglomerative clustering of cell lines in response to PARP

583   inhibition reveals 4 distinct clusters. (C) Clustered sensitivity to PARP inhibition showed

584   compound-specific responses, particularly in Cluster 3, which shows equal sensitivity to the

585   pan-sensitive Cluster 1 in talazoparib, similar sensitivity to Cluster 1 in niraparib and

586   olaparib, but relative resistance in comparison to Cluster 1 in rucaparib and veliparib. (D)

587   Selection of genes showing differences in essentiality across clusters. Columns denoted by

588   arrows correspond to genes found to differentially affect response to PARP inhibition

589   between Group A and Group B inhibitors.

590

591

592

593

594

595

596
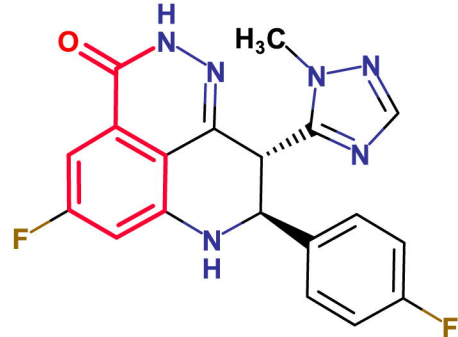
Talazoparib
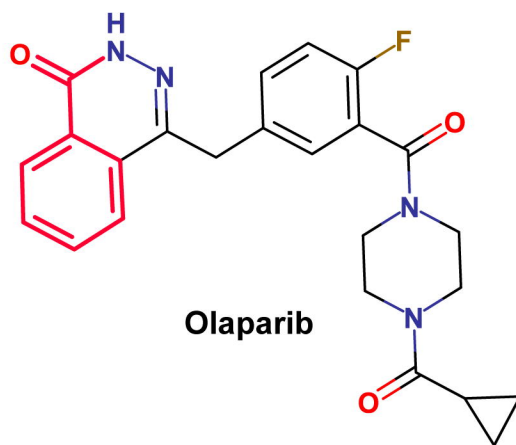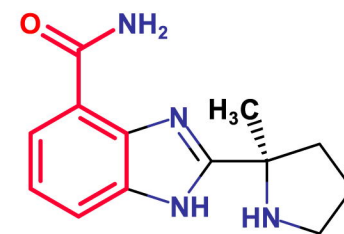
Olaparib

Veliparib
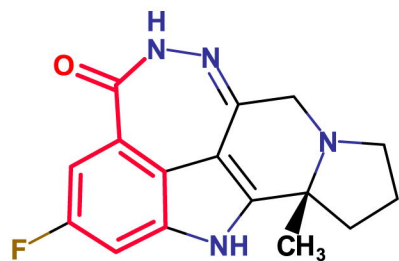
Rucaparib
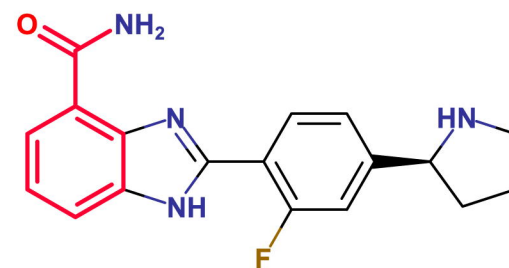
A-966492
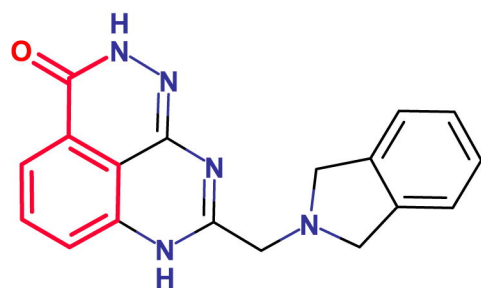
KU-005894

E-7449
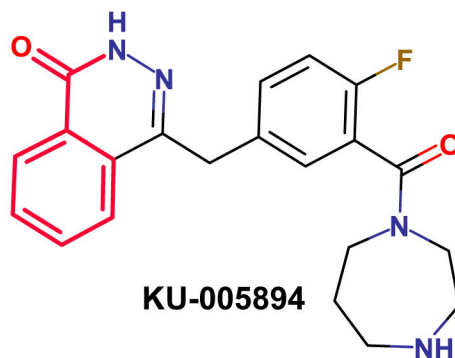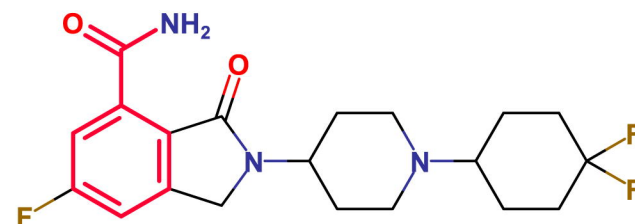
NMS-P118
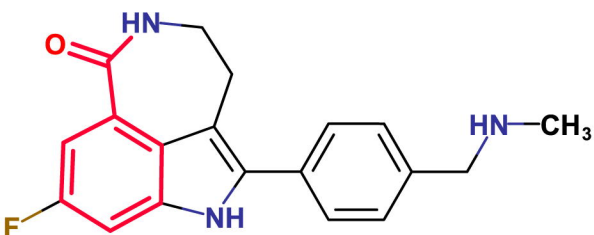
BGB-290

AG-1436

Niraparib

A

PARylation (Normalized) vs Olaparib (nM)

- ■ -MMS
- ▨ +MMS

Olaparib (nM)

DMSO | Olaparib (nM): 8 | 25 | 75

- MMS
+ MMS

B

PARylation Inhibition via Immunoblot Assay

KU-0058948
A-966492
E-7499
AG-1481
Niraparib
Veliparib
Olaparib
Rucaparib
Talazoparib

-10 -9 -8 -7 -6 -5

C

PARP-1 Trapping via Fluorescence Polarization

KU-0058948
NMS-P118
A-966492
E-7499
AG1481
Niraparib
Veliparib
Olaparib
Rucaparib
Talazoparib

-11 -10 -9 -8 -7 -6 -5

LogEC50

D

PARP-1 Trapping vs Inhibition of PARylation

E-7499
AG-1481
Veliparib
Olaparib
A-966492
KU-0058948
Niraparib
Rucaparib
Talazoparib

$R^2 = 0.1058$

PARylation LogEC50

PARP-1 Trapping LogEC50

A

Wild-Type Growth Inhibition vs Inhibition of PARylation

Wild-Type Growth Inhibition vs PARP-1 Trapping Potency
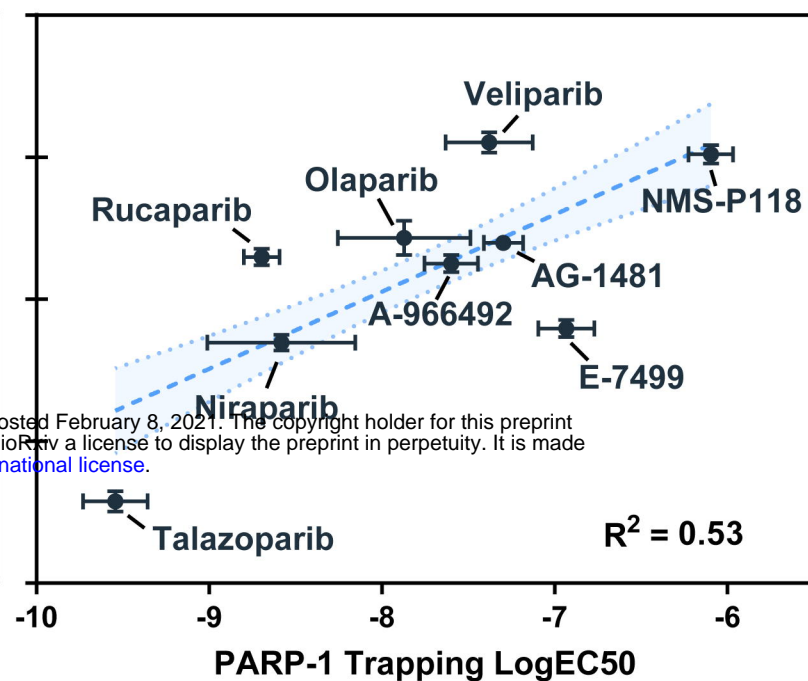
B

BRCA2 -/- Growth Inhibition vs Inhibition of PARylation
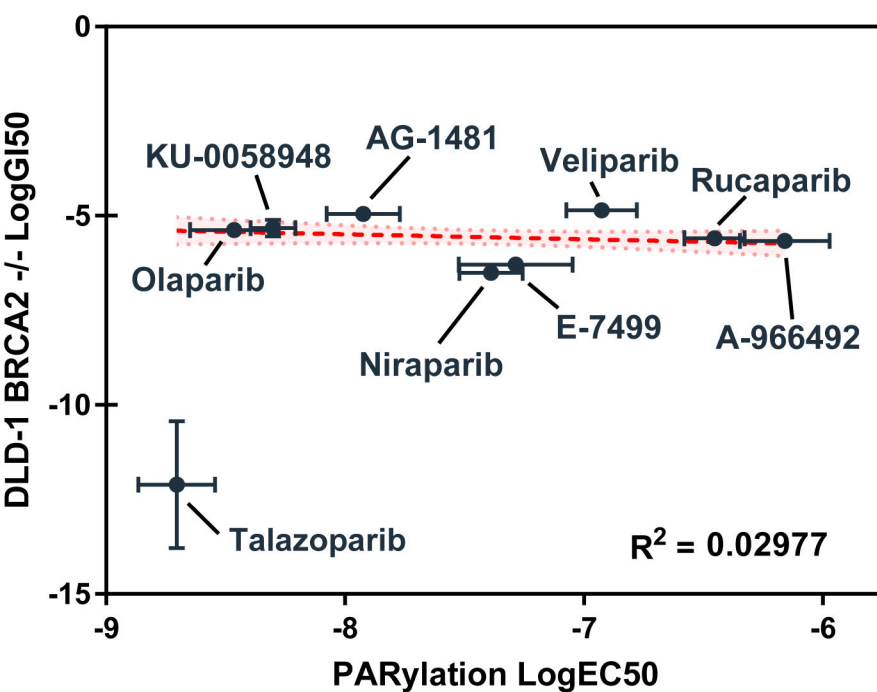
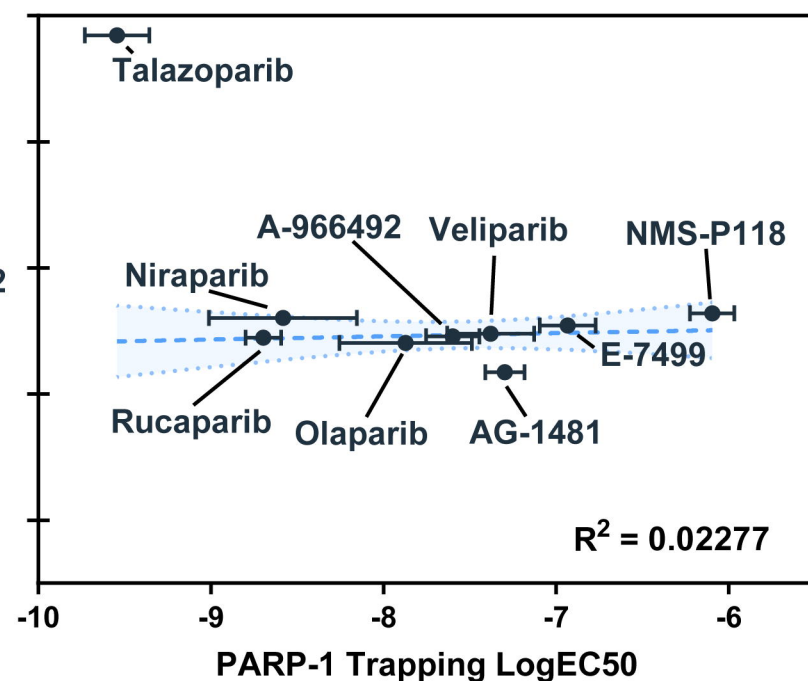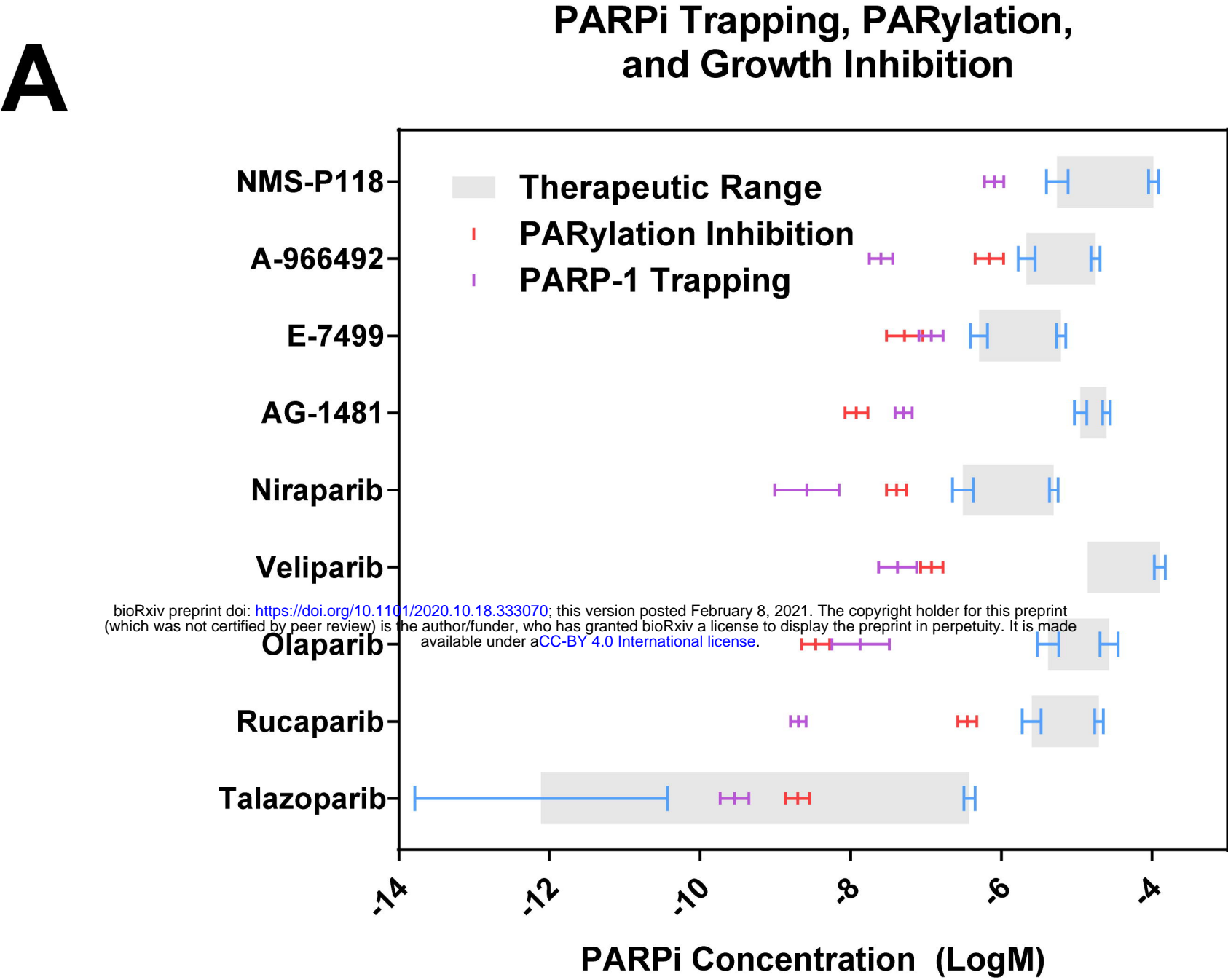**BRCA2 -/- Growth Inhibition vs PARP-1 Trapping Potency**

C
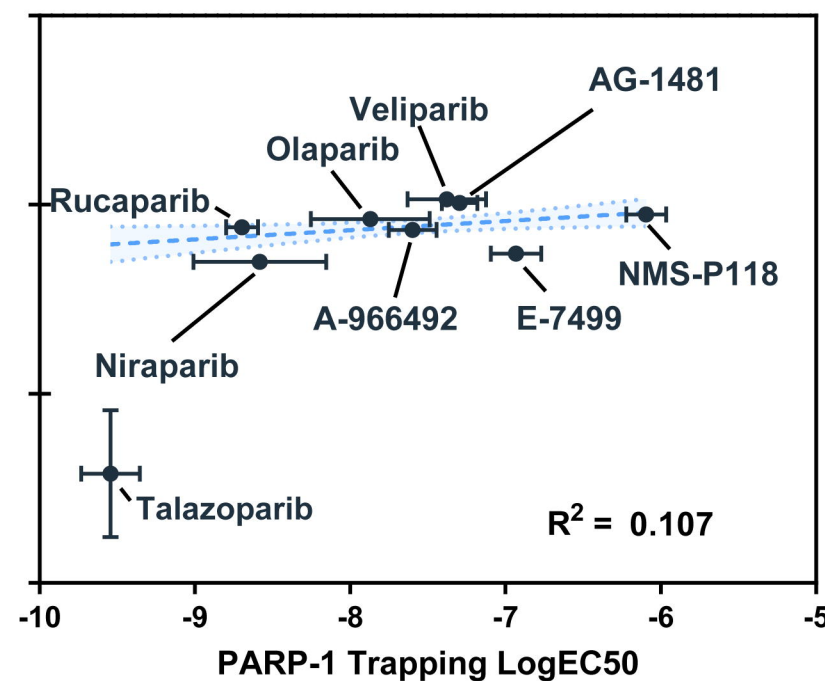
Synthetic Lethality vs Inhibition of PARylation
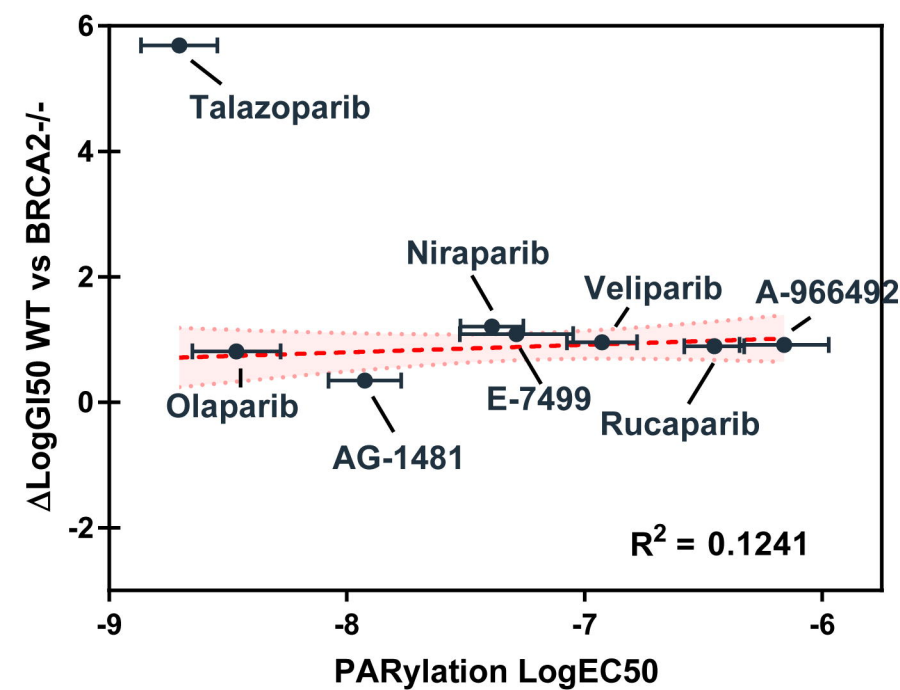
Synthetic Lethality vs PARP-1 Trapping Potency
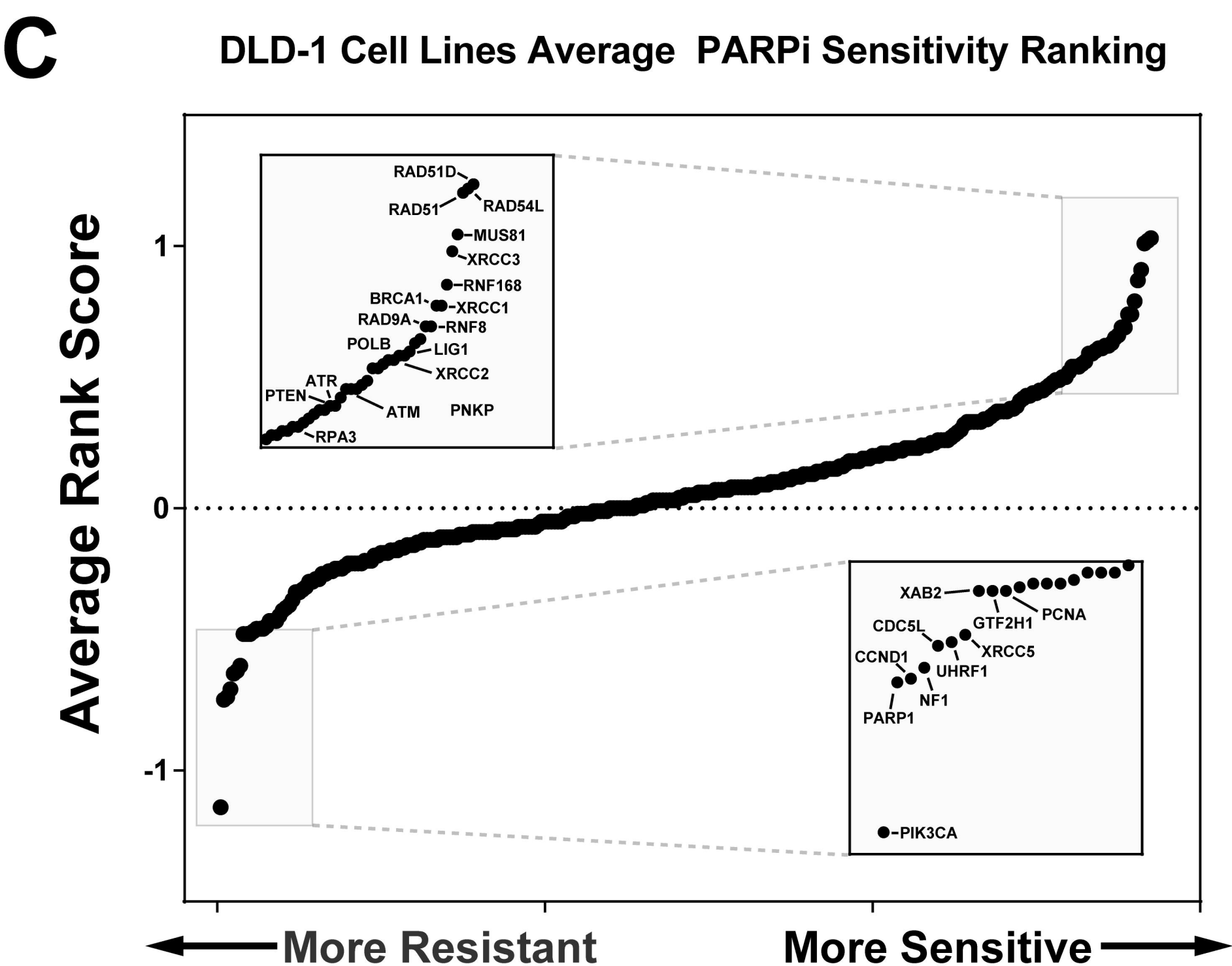
A

PARPi Trapping, PARylation, and Growth Inhibition

NMS-P118

A-966492

E-7499

AG-1481

Niraparib

Veliparib

Olaparib

Rucaparib

Talazoparib

Therapeutic Range
PARylation Inhibition
PARP-1 Trapping

PARPi Concentration (LogM)

B

PARP Inhibitor	Trapping LogIC50	PARylation LogIC50
Talazoparib	-9.543	-8.705
Rucaparib	-8.696	-6.454
Olaparib	-7.871	-8.464
Veliparib	-7.379	-6.926
Niraparib	-8.582	-7.389
AG1481	-7.296	-7.924
E-7499	-6.932	-7.286
A-966492	-7.598	-6.160
NMS-P118	-6.095	-
KU-0058948	-8.343	-8.302

C

DLD-1 Cell Lines Average PARPi Sensitivity Ranking

Average Rank Score

RAD51D
RAD54L
RAD51
MUS81
XRCC3
RNF168
BRCA1
RAD9A
XRCC1
RNF8
POLB
LIG1
XRCC2
ATR
PTEN
ATM
PNKP
RPA3

XAB2
GTF2H1
PCNA
CDC5L
XRCC5
CCND1
UHRF1
NF1
PARP1
PIK3CA

More Resistant   More Sensitive

D

Principal Component 2

Niraparib
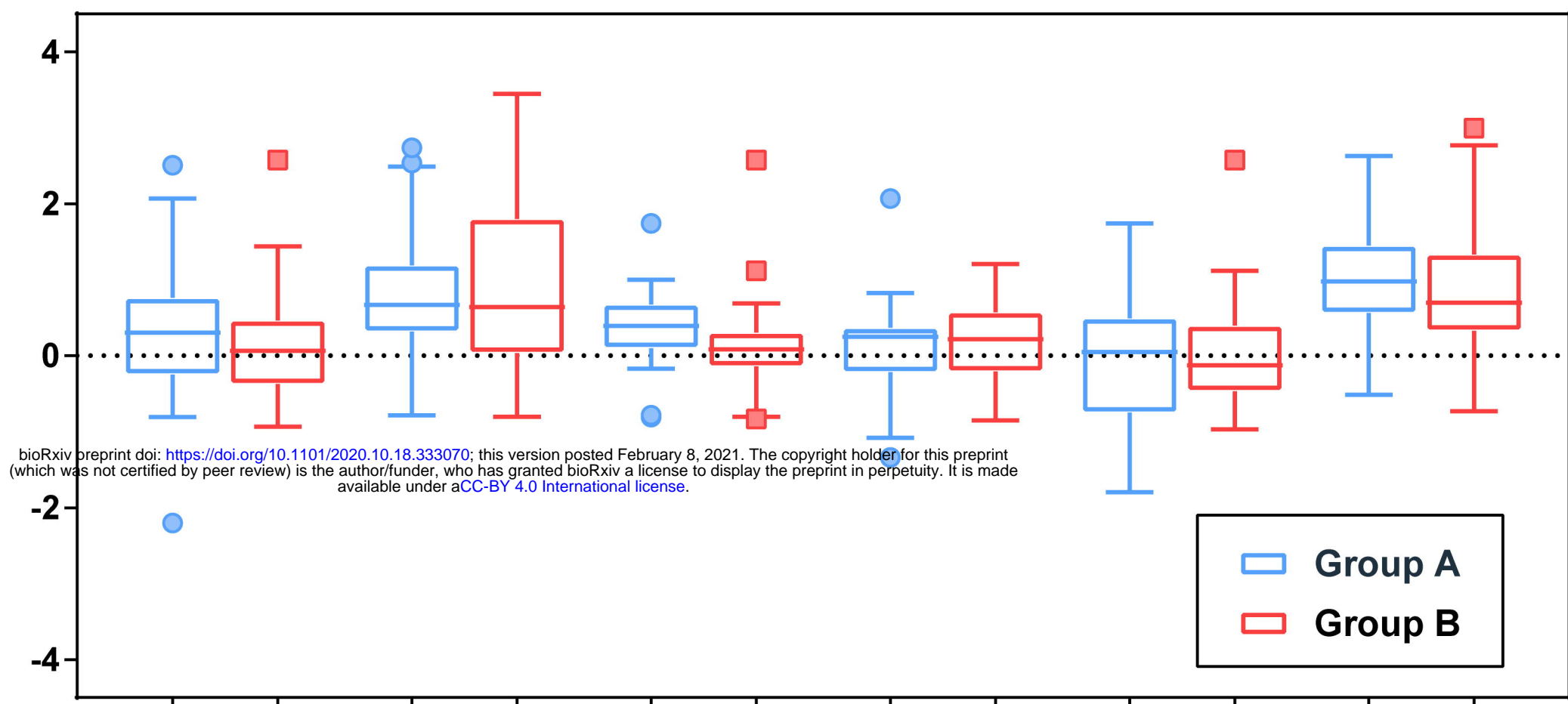
Talazoparib

Rucaparib

Veliparib

Olaparib

Group A
Group B

Principal Component 1

A

Rank Score Distribution By Gene Set

Group A
Group B

B

Base Excision Repair-Associated Proteins

Rank Score

**

****

*

***

Group A
Group B

- Log10(p)

p = 0.05

APEX1 APEX2 FEN1 LIG1 LIG3 MBD4 MPG MUTYH NEIL1 NEIL2 NEIL3 NTHL1 OGG1 PARP1 PARP2 PARP3 PCNA POLB POLD1 POLD2 POLD3 POLD4 POLE POLE2 POLE3 POLE4 POLL SMUG1 TDG UNG XRCC1

A — DLD-1 WT Short-Term Viability

ΔLogEC50 vs sgRNA Target (PARP1, LIG3, XRCC1)
Legend: Talazoparib, Olaparib, Niraparib, Veliparib, Rucaparib

B — DLD-1 WT Short-Term Viability

ΔLog(siRNA/RISC-Free) vs siRNA Target (PARP1, LIG3, XRCC1)
Legend: Talazoparib, Olaparib, Niraparib, Veliparib, Rucaparib

C — U2-OS Short-Term Viability

ΔLogEC50 vs sgRNA Target (PARP1, LIG3, XRCC1)
Legend: Talazoparib, Olaparib, Niraparib, Veliparib, Rucaparib